THINK INDIA JOURNAL

ISSN:0971-1260
Vol-22- Issue-14-December-2019

A Different Approach To Represent The Reinforcement Layers Of Tyre For Finite Element Analysis

[1] M. Mondal, [2] P. Ghosh, [3] S. Chattopadhyay, [4] R. Mukhopadhyay
[1] Hari Shankar Singhania Elastomer & Tyre Research Institute,437, Hebbal Industrial Area, Mysuru-570016, Karnataka, India, [2] Hari Shankar Singhania Elastomer & Tyre Research Institute,437, Hebbal Industrial Area, Mysuru-570016, Karnataka, India, [3] Indian Institute of Technology Kharagpur, West Medinipur-721302, West Bengal, India, [4] Hari Shankar Singhania Elastomer & Tyre Research Institute,437, Hebbal Industrial Area, Mysuru-570016, Karnataka, India
[1] mrinmoy.mondal@jkmail.com

Abstract— A finite element model is developed to predict the macro properties like radial, lateral, longitudinal, torsional stiffness and force & moment characteristics in steady state rolling condition for pneumatic tyres. This model combines accuracy together with a substantially reduced computational effort. The cord reinforced rubber sections such as body ply, belt, and cap-strip are modelled with orthotropic composite material properties, and rubber sections are modelled with the hyperelastic material model. In another finite element model cord reinforced rubber sections are represented with rebar layer embedded in hyperelastic rubber material and other sections are same as the previous model. The results from this finite element models are then compared with the experimental results. It is concluded that the results obtained from the finite element model with orthotropic composite material properties give more accurate results with remarkably reduced computational effort than the finite element model with embedded rebar layer in its reinforcement layers.

Index Terms— Tyre, Finite element analysis, Stiffness, Rebar layer, Composite.

1. INTRODUCTION

Tyres in an automobile play a very crucial role in ensuring lateral & longitudinal stability, comfort and safety. New generation automobiles demand continuous improvement in these characteristics that poses great challenges to the tyre designers. Finite Element Analysis (FEA) technique is proven to be a great saviour in terms of design cycle time optimization and knowledge proliferation. FEA is used extensively in tyre development process to keep pace with faster development in automobile industry. With the advent of powerful computational resources as well as availability of commercial software, the simulation turnaround time has been reduced substantially in recent times. It prompts tyre designers in attempting to predict more and more complex tyre performance characteristics to take advantage of shorter simulation cycle time. During the tyre design stage, simulations are generally carried out to predict various performance characteristics which include stiffness (lateral, radial, longitudinal and torsional), Force & Moment (F&M), temperature distribution etc. The influence of design and material attributes on these performance characteristics are of paramount interest. Very often these attributes are varied to achieve desired performance characteristics.

Tyre is a composite product consists of rubber compound, organic and steel cords. While performing FE analysis of tyre for performance prediction, material modelling is one of the key steps. Rubber compounds are generally modelled using hyperelastic material models. Among the available hyperelastic model, Yeoh model is widely used for modelling of various rubber components in tyre FE analysis because of its advantage over other models [1]. In case of organic and steel cords, there are mainly two modelling approaches, which can be employed. One approach, models each cords separately by rebar element embedded in rubber matrix [2], [3], [4], [5]. The other approach models rubber and cords together wherein

ISSN:0971-1260
Vol-22- Issue-14-December-2019

properties are defined according to the rule of mixture [6]. As the cord rubber composite is orthotropic in nature, the orthotropic material properties can be applied using shell elements for tyre FEA [7], [8], [9], [10], [11] or using solid elements [11], [12]. For prediction of stress distribution, heat generation etc., usage of continuum elements will be more appropriate in comparison with shell element. With this background, present work aims to strike a balance between predictability and computational time requirement. In this work, FE analysis is carried out using (a) rebar layer and (b) composite material model. In both the cases continuum elemnts were used. Results and computational time for both the methods will be compared in diftterent tyres sizes.

2. FINITE ELEMENT MODELLING

2.1 Model Generation

Three different passenger car radial tyre sizes (135/70R12, 175/65R14 and 205/60R16) have been chosen for the present study. Exploiting the symmetry, only half cross section of tyre was modelled in 2-D. There are two different modelling strategies were used which are termed as Rebar Layer Model and Composite Model. By revolving and reflecting the 2-D elements full 3-D tyre is generated which is identical for both the model.

2.1.1. Rebar Layer Model:

The CAD layout of half tyre cross section is discretized in small portions as per the desired element. Then using a commecial preprocessor all the nodes and corresponding elements are created. Different node and element sets are created to assigned material properties. The rubber portion (matrix) of all the tyre components are modelled using 4 nodded and 3 nodded axisymmetric continuum elements with a twist. Yeoh material model [13] is used to reperesent the materail properties of the rubber matrix. Tyre reinforcement members (organic and steel cords) are modelled using axisymmetric two nodded elements embedded on continuum matrix. Here the cross-sectional area, the spacing between the cords, angle of the cord directions is assigned. Young's modulus and Poisson's are assigned as material property for organic and steel cords.

Symmetric model generation technique [14] has been used to generate the three-dimensional tyre model from the two-dimensional axisymmetric model. 6-nodded linear triangular prism and 8 nodded linear brick element with hybrid formulation three-dimensional model generation. The rebar layer in three-dimensional tyre model are modelled with 4-nodded quadrilateral reduced integration element. The road has been modeled as a rigid body using R3DR4 element [14]. Node to surface direct contact is defined between the road and tyre surface. For the sake of simplicity, tread pattern geometry is not considered in this analysis. The modelling flowchart is shown in Fig. 1.

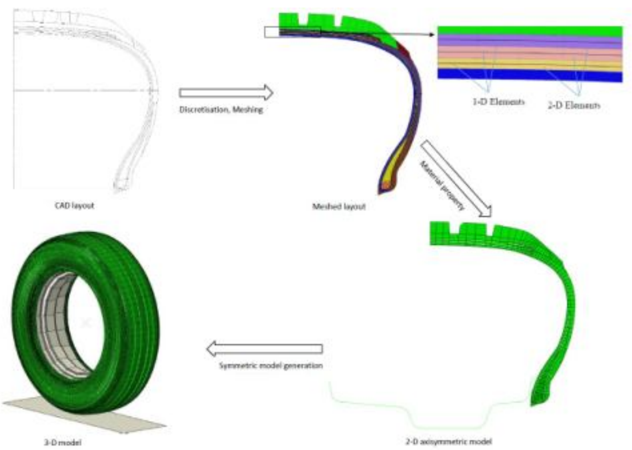

Fig. 1: Modelling flowchart of rebar layer model

2.1.2. Composite Model:

In this model, the rubber matrix of non-reinforced layers like tread, sidewall etc. are modelled in a similar way like the Rebar Layer Model All the reinforcement layers (body ply, belts, cap-strips, etc.) are considered as a composite of cord and rubber. The reinforcement layers are meshed with 4 nodded axisymmetric continuum elements with a twist. Material orientation are defined at the reinforcement layers shown in

ISSN:0971-1260
Vol-22- Issue-14-December-2019

Fig. 2. This composite has different mechanical properties in the direction of cord than the other two directions where the mechanical properties are same. Thus, this cord-rubber composite is an orthotropic material [7], [8], [9], [10], [11]. To define this material property for finite element analysis in Abaqus, several engineering constants has been used, which are calculated according to the following formulas:

$$E_1 = [E_C \times \mathrm{V}_C] + [E_R \times (1\text{-}\ \mathrm{V}_C)] \qquad (1)$$

$$E_2 = E_3 = E_R \times \frac{(1{+}2\mathrm{V_C})}{(1\text{-}\mathrm{V_C})}$$

(2)

$$\nu_{12} = [V_C \times \nu_C] + [(1 - V_C) \times \nu_R]$$

(3)

$$\nu_{21} = \frac{(\nu_{12} \times \mathrm{E}_2)}{E_1} \qquad (4)$$

$$\nu_{23} = (0.98 - \nu_{21}) \qquad (5)$$

$$G_{12} = G_{13} = \frac{0.25 \times \sqrt{E_1 \times E_2}}{2 \times (1 + \sqrt{\nu_{12} \times \nu_{21}}}$$

(6)

$$G_{23} = G_R$$

where C denotes cord and R denotes rubber; V_C is volume fraction of cord in a rubber matrix. E1, E2, and E3 are Young's modulus of the composite in direction 1, 2 and 3 respectively. G12, G13, and G23 are the shear modulus of plane 12, 13 and 23 respectively. ν12, ν12 and ν23 are the Poisson's ratio of plane 12, 13 and 23 respectively. ER=6×C10, $V_C = \frac{EPI \times H}{A}$ [EPI=ends per inch, A= cross-sectional area of cord, H= thickness of the reinforcement layer]. The directions 1, 2 and 3 are according to Fig. 2. Equation (1), (2), (3), (4) is based on the equation proposed by Halpin and Tsai [6], (5) and (7) are based on the equations used by J Pelc [8]. Under shear deformation of the composite the local material orientations changes in Abaqus, so the direction 1 shift from the direction of cord. Hence, in (6) the shear modulus of plane 12 and plane 13 are used in such a way that it restricts the shifting of material orientation direction 1 from the direction of cord and also maintains accuracy of results.

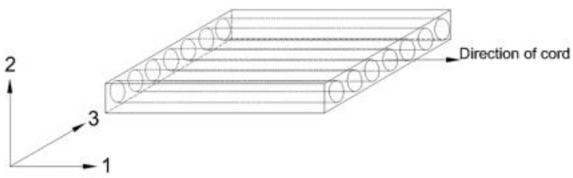

Fig. 2: Directions of the composite

The 3-D model generation is identical as the rebar layer model. The modelling flowchart is shown in Fig. 3.

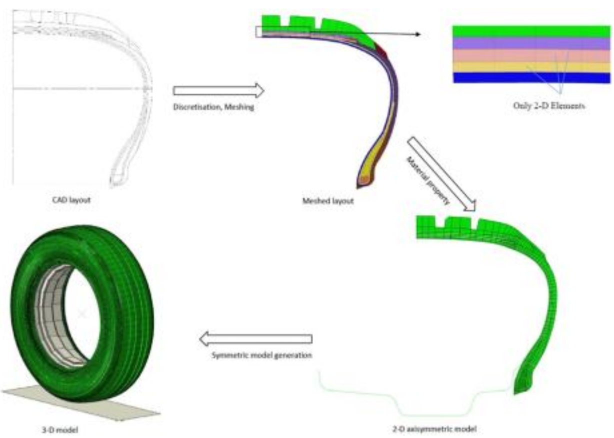

Fig. 3: Modelling flowchart of composite model

2.2. Boundary Conditions:

A constant uniformly distributed pressure is applied in the inner surface of the tyre whereas the reference node of the rim is fully constrained. All the loads are applied through the road. In case of steady state rolling analysis the angular and linear velocity has been applied on the tyre and road respectively.

ISSN:0971-1260
Vol-22- Issue-14-December-2019

Loads and boundary conditions of particular type of simulation has been described in next section.

2.3. Solution Strategy:

We have followed identical simulation procedure for rebar layer model and composite model.

2.3.1. Axisymmetric Inflation Analysis:

First, a node located in the middle of the bead has been moved inside the rim by applying displacement boundary condition so that the bead part goes inside the rim. After that, the rim has been fully constrained, and the nodes of the symmetric line have been partially constrained. Then the specified inflation pressure has been applied as distributed surface pressure. The specified inflation pressures of the tyres are given in Table *I*.

Table *I*: Inflation pressures

Tyre Size	**Inflation Pressure (MPa)**
135/70R12	0.241
175/65R14	0.210
215/60R16	0.230

2.3.2. Radial Load Deflection Analysis:

For radial load deflection simulation, first the tyre has been inflated to the specified inflation pressure, then the rigid body road has been moved towards the tyre so that a contact is established between the road and tyre. Then the specified radial load has been applied. The inflation pressure and radial load of this step are provided in Table *II*.

Table *II*: Inflation pressures and radial loads

Tyre Size	Inflation Pressure (MPa)	Radial Load (N)
135/70R12	0.241	2845
175/65R14	0.210	2950
215/60R16	0.230	3956

2.3.3. Lateral, Longitudinal and Torsional Load Deflection Analysis:

To simulate the lateral and longitudinal load deflection, the road has been displaced in a lateral and longitudinal direction respectively by applying the displacement boundary condition along with the previous radial load and inflation pressure. In the lateral direction, the road has been displaced to 63.5 mm, and in the longitudinal direction, the road is displaced to 30.48 mm. To simulate the torsional load deflection, the road is rotated to 5^{O} along the perpendicular axis of the road with the specified radial load and inflation pressure.

2.3.4. Force and Moment Analysis:

For tyre rolling simulation, Eulerian-Lagrangian approach [15], [16] is used. An appropriate rotational and linear motion has been given to the tyre along with the specified radial load and inflation pressure. The rotational speed is chosen in such a way that there should not be any slip between road and tyre surface while tyre is running straight ahead. The linear motion given for this simulation is 10 km/hr. For cornering simulation, the direction of linear motion of the tyre has been changed according to the slip angle. The cornering condition is shown in Fig. 4.

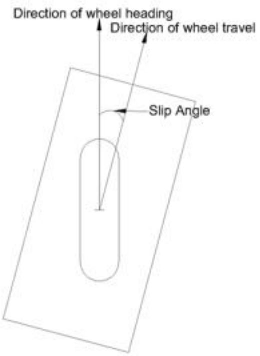

Fig. 4: Cornering of tyre

ISSN:0971-1260
Vol-22- Issue-14-December-2019

3. TYRE PROPERTY MEASUREMENT:

The 175/65R14 tyre is tested for inflated dimensions, radial stiffness, lateral stiffness, longitudinal stiffness, torsional stiffness, and force & moment characteristics. The inflated dimensions are measured using Vernier scale, the radial stiffness, lateral stiffness, longitudinal stiffness, torsional stiffness are measured in a Tyre Universal Test Machine. Force & moment characteristics are measured in a flat belt Force & Moment machine.

4. RESULTS AND DISCUSSION

The results of this study is divided in two parts. The first portion compares the results of finite element models with the experimental result to check the accuracy of the models. And the second portion is to confirm the repeatability of the model. Two more tyre size have been modeled and results were compared.

4.1. Comparison between the Experimental Results and Results from FE Analysis of Tyre 175/65R14

Radial Stiffness: The radial load-deflection plots of 175/65R14 tyre is shown in Fig. 5. The radial stiffness of the FE models and experimental results are given in Table *III*. The radial stiffness of Composite Model is slightly higher than the experimental result, and for Rebar Layer Model, the stiffness is lower than the experimental result. The radial stiffness of Composite Model is closer to the experimental result than Rebar Layer Model.

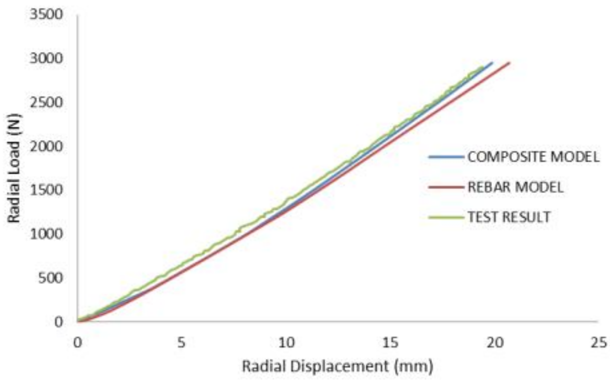

Fig. 5: Radial Load vs Radial Displacement of 175/65R14

Table *III*: Radial stiffness of tyre 175/65R14:

Radial Stiffness (N/mm)		Diff. from Exp. Result
Composite model	150.92	0.46%
Rebar layer model	141.82	-5.59%
Test Data	150.22	-

Lateral Stiffness: The lateral load-deflection plots of 175/65R14 tyre is shown in Fig. 6. The lateral stiffness of the FE models and experimental result is given in Table *IV*. The Lateral Stiffness for both Composite and Rebar Layer Model is lower than the experimental result. The lateral stiffness of Composite Model is closer to the experimental result than Rebar layer model.

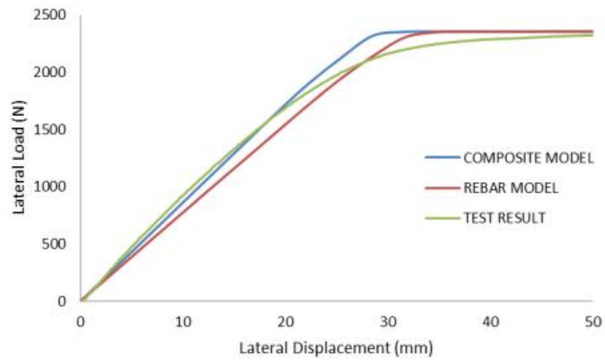

Fig. 6: Lateral Load vs Lateral Displacement of 175/65R14

Table *IV*: Lateral stiffness of tyre 175/65R14:

lateral stiffness (N/mm)		Diff. from Exp. Result
Composite model	86.17	-5.92%
Rebar layer model	77.45	-15.44%
Test Data	91.59	-

Longitudinal Stiffness: The longitudinal load-deflection plots of 175/65R14 tyre is shown in Fig. 7. The longitudinal stiffness of the FE models and experimental result is provided in Table *V*. The longitudinal stiffness of Composite Model is higher than the experimental result, and the longitudinal stiffness of Rebar layer model is lower than the experimental result. The difference of longitudinal stiffness between Composite Model and experimental result is slightly higher than the difference between Rebar layer model and Experimental result.

ISSN:0971-1260
Vol-22- Issue-14-December-2019

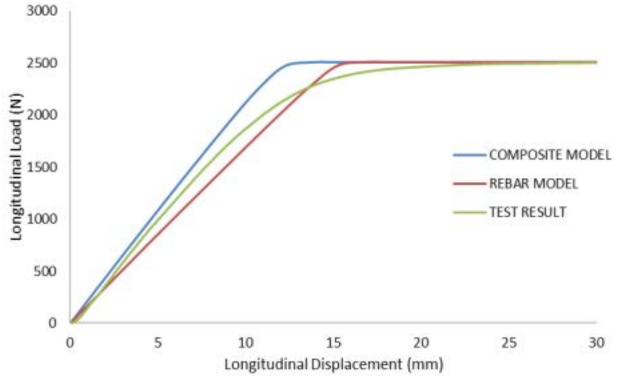

Fig. 7: Longitudinal Force vs Longitudinal Displacement of 175/65R14

Table *V*: longitudinal stiffness of tyre 175/65R14

Longitudinal stiffness (N/mm)		Diff. from Exp. Result
Composite model	210.90	12.23%
Rebar layer model	166.35	-11.48%
Test Data	187.91	-

Torsional Stiffness: The torque vs. angle of torsion plots of 175/65R14 tyre is shown in Fig. 8. The torsional stiffness of the FE models and experimental result is given in Table *VI*. The torsional stiffness values from both the FE model is close to the experimental result.

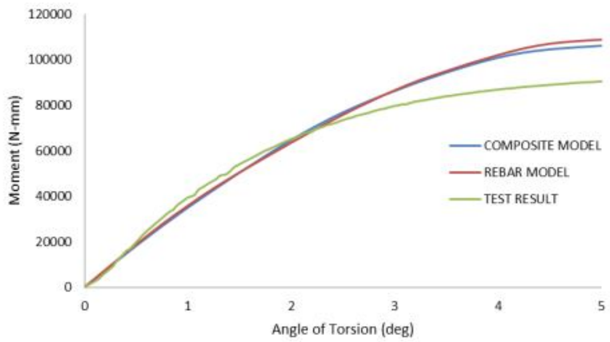

Fig. 8: Torque vs Rotation of 175/65R14

Table *VI*: Torsional stiffness of tyre 175/65R14:

Torsional stiffness (N-mm/°)		Diff. from Exp. Result
Composite model	32417.69	-0.62%
Rebar layer model	31766.64	-2.62%
Test Data	32620	-

Cornering Stiffness: The lateral force vs. slip angle plots is shown in Fig. 9, the cornering Stiffness of FE models and experimental result is provided in Table *VII*. The curves of Composite Model and Rebar layer model are very similar, but the cornering stiffness value of the Composite Model is more close to the experimental result than the Rebar layer model.

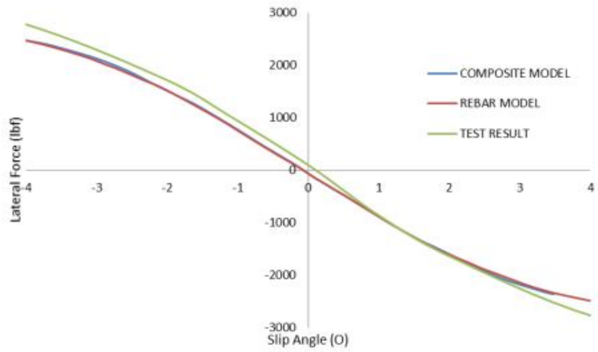

Fig. 9: Lateral Force vs Slip Angle of 175/65R14

Table *VII*: Cornering stiffness of tyre 175/65R14:

Cornering stiffness (N/^{O})		Diff. from Test Data
Composite model	827.35	-7.93%
Rebar layer model	818.06	-8.97%
Test Data	898.64	-

4.2. Comparison between the results (from FE Analysis) of Composite Model and Rebar layer model of tyre size 135/70R12, 175/65R14, and 215/60R16

Radial Stiffness: The radial stiffness of tyre 135/70R12, 175/65R14 and 215/60R16 is provided in Table *VIII*. The analysis time taken by the Composite model as compared to Rebar layer model is given in Table *IX*. For all the tyres, a difference of the radial stiffness between Composite Model and Rebar Layer Model is similar, and for each tyre, the Composite Finite Element Model has taken less computational time.

ISSN:0971-1260
Vol-22- Issue-14-December-2019

Table *VIII*: Radial stiffness

Tyre Size	Radial Stiffness		
	Composite Model (N/mm)	Rebar layer model (N/mm)	Difference of Composite Model from Rebar layer model (%)
135/70R12	143.85	135.21	6.39
175/65R14	150.92	141.82	6.41
215/60R16	203.41	190.78	6.61

Table *IX*: Comparison of computational time

Tyre Size	Computational Time(Sec.)		
	Composite Model	Rebar layer model	Time taken by composite model as % of time taken by Rebar layer model
135/70R12	1696	2069	81.97
175/65R14	3887	4233	91.82
215/60R16	1506	1776	84.79

Lateral Stiffness: The lateral stiffness of tyre 135/70R12, 175/65R14 and 215/60R16 is given in Table *X*. The analysis time taken by the Composite model as compared to Rebar layer model is given in Table *XI*. When the results from the finite element models of 175/65R14 size tyre were compared with the experimental result, it was found that the results from both the FE model were less than that of the experimental result.

Table *X*: Lateral stiffness

Tyre Size	Lateral Stiffness		
	Composite Model (N/mm)	Rebar layer model (N/mm)	Difference of Composite Model from Rebar layer model (%)
135/70R12	68.02	59.28	14.73
175/65R14	86.17	77.45	11.25
215/60R16	110.64	103.35	7.05

Table *XI*: Comparison of computational time

Tyre Size	Computational Time(Sec.)		
	Composite Model	Rebar layer model	Time taken by composite model as % of time taken by Rebar layer model
135/70R12	2288	5514	41.49
175/65R14	1535	2212	69.39
215/60R16	1719	4250	40.44

Longitudinal Stiffness: The longitudinal stiffness of tyre 135/70R12, 175/65R14 and 215/60R16 is given in Table *XII*. The analysis time taken by the Composite model as compared to Rebar layer model is provided in Table *XIII*. For 135/70R12 and 215/60R16 size tyre the result difference trend is similar to 175/65R14 size tyre. Previously it was found that the longitudinal stiffness from the composite model was higher than the experimental result, and the longitudinal stiffness value from the rebar layer model was lower than the experimental result, that is why the difference between the results of FE model is higher. For each tyre size, the composite

ISSN:0971-1260
Vol-22- Issue-14-December-2019

model has taken less computational time than that of the rebar layer model.

Table *XII*: Longitudinal stiffness

Tyre Size	Longitudinal Stiffness		
	Composite Model (N/mm)	Rebar layer model (N/mm)	Difference of Composite Model from Rebar layer model (%)
135/70R12	193.72	148.63	30.33
175/65R14	210.90	166.35	26.78
215/60R16	256.90	199.47	28.79

Table *XIII*: Comparison of computational time

Tyre Size	Computational Time (Sec.)		
	Composite Model	Rebar layer model	Time is taken by composite model as % of time taken by Rebar layer model
135/70R12	1040	1300	80.00
175/65R14	903	1484	60.85
215/60R16	1031	1401	73.59

Torsional Stiffness: The torsional stiffness of tyre 135/70R12, 175/65R14 and 215/60R16 have been shown in Table *XIV*. The analysis time taken by the Composite model as compared to Rebar layer model have been shown in Table *XV*. The torsional results from both of the FE models are very close. For every case the difference is less than 5%. For each tyre size, the composite model has taken less computational time than that of the rebar layer model.

Table *XIV*: Torsional stiffness

Tyre Size	Torsional Stiffness		
	Composite Model (N-mm/°)	Rebar layer model (N-mm/°)	Difference of Composite Model from Rebar layer model (%)
135/70R12	19973.73	19037.13	4.92
175/65R14	32417.35	31766.59	2.04
215/60R16	52481.47	54292.54	-3.33

Table *XV*: Comparison of computational time

Tyre Size	Computational Time (Sec.)		
	Composite Model	Rebar layer model	Time taken by composite model as %of time taken by Rebar layer model
135/70R12	1123	1394	80.55
175/65R14	1034	1537	67.27
215/60R16	1236	1299	95.15

Cornering Stiffness: The cornering stiffness of tyres 135/70R12, 175/65R14 and 215/60R16 is shown in Table *XVI*. The analysis time taken by the Composite model as compared to Rebar layer model is provided in Table *XVII*.

ISSN:0971-1260
Vol-22- Issue-14-December-2019

Table *XVI*: Cornering stiffness

Tyre Size	Cornering Stiffness		
	Composite Model (N/^{o})	Rebar layer model (N/^{o})	Difference of Composite Model from Rebar layer model (%)
135/70R12	462.97	415.55	11.41
175/65R14	827.35	818.06	1.14
215/60R16	816.29	821.27	0.60

Table *XVII*: Comparison of computational time

Tyre Size	Computational Time(Sec.)		
	Composite Model	Rebar layer model	Time is taken by composite model as %of Rebar layer model
135/70R12	7727	20628	37.46
175/65R14	8898	9913	89.76
215/60R16	10286	22934	44.85

Table *XVIII*: Comparison of overall computational time taken by FE Models for all the analysis:

Tyre Size	Overall computational time was taken (sec.)		Time taken by composite model as %of time taken by Rebar layer model
	Composite Model	Rebar layer model	
135/70R12	15659	33236	47.11%
175/65R14	19215	24066	79.84%
215/60R16	20849	37000	56.35%

5. CONCLUSION

The results from both the finite element models have been compaired with the experimental result of tyre 175/65R14. For most of the results from composite model is more accurate than the rebar layer model. The simulation results of 135/70R12 & 215/60R16 also proves the repeatability of the composite model. For all the cases the composite model is taking significantly lower computational effort or analysis time than that of the rebar layer model. For composite models, the savings of analysis time is varying from 20.16% to 52.89%. Hence the composite model is giving more accurate results with less computational effort.

6. REFERENCES

[1] P. Ghosh, A. Saha, P.C. Bohara and R. Mukhopadhyay "Material Property Characterization for Finite Element Analysis of Tyre", Rubber World, Vol, 233, No.4, January, 2006.

[2] E. Tonuk, Y. S. Unlusoy, "Simple Analytic Tyre Models for Vehicle Dynamic Simulations, Part I: Models." 7th National Machine Theory Symposium, İstanbul, pp. 606-615, 1995.

[3] K.V.N. Rao, R. K. Kumar, P. C. Bohara, C. P. Mouli, "Dynamic Analysis Of Tyre Cornering Behavior Using Explicit Finite Element Code," Proceedings of Twenty First Southeastern Conference On Theoretical And Applied Mechanics, Orlando, Florida, 2002.

[4] K.V.N. Rao, R. K. Kumar, P. C. Bohara, C. P. Mouli, "Transient Finite Element Analysis of Tire Dynamic Behavior," Tire Science and Technology, TSTCA, Vol. 31, No. 2, 104-127, 2003.

[5] K. Kabe, M. Koishi, "Tyre cornering Simulation Using Finite Element Analysis," Journal of Applied Polymer Science, Vol 78, 1566-1572, 2000.

[6]http://www.mse.mtu.edu/~drjohn/my4150/ht/ht.html

ISSN:0971-1260
Vol-22- Issue-14-December-2019

[7] M. Koishi, K. Kabe, M. Shiratori, "Tyre Cornering Simulation Using an Explicit Finite Element Analysis Code," Tyre Science and Technology, TSTCA, Vol26, No.2, 109-119, 1998.

[8] J. Pelc, "Material Modeling in Cord Rubber Structures," KGK Kautschuk Gummi Kunststoffe 53. Nr. 10/2000 Poland, 561-565, 2000.

[9] M. Hauke, R. Hanley, D. Crolla, "Tyre FE Modeling for Misuse Situations", SAE 2001-01 0748, SAE World Congress, Detroit, 2001

[10] O. A. Olatunbosun, A. M. Burke, "Material Property Derivation for Finite Element Modeling of Tires", Presented at the 16th Annual Meeting of the Tire Society, 1997.

[11] M. H. R. Ghoreishy, "Finite Element Analysis of a 6.45-14 Bias Tyre Under Contact Load", Iranian Polymer Journal, Vol 10, 53-58, 2001.

[12] J. Pelc, "An Attempt to Improve the Axisymmetric Model of a Pneumatic Tyre" Technical Sciences, 233-239, 2010.

[13] O. H. Yeoh, "Some Forms of the Strain Energy Function for Rubber", Rubber Chemistry and Technology, Vol. 66, pp. 754-771, 1993

[14] ABAQUS Documentation, Version 6.14, 2014

[15] P. Ghosh, A. Saha, Mukhopadhyay, R., Bohara, P., et al., "Optimization of Tyre Design Parameters Through Finite Element Analysis and Correlation with Performance," SAE Technical Paper 2007-26-043, 2007.